NASA TECHNICAL NOTE

NASA TN D-4777

NASA TN D-4777

EFFECT OF RESIDUAL STRESS ON FRACTURE STRENGTH OF AISI 301 STAINLESS-STEEL AND Ti-5Al-2.5Sn ELI TITANIUM CRACKED THIN-WALL CYLINDERS

by Frederick D. Calfo

Lewis Research Center
Cleveland, Ohio

NATIONAL AERONAUTICS AND SPACE ADMINISTRATION • WASHINGTON, D. C. • SEPTEMBER 1968

NASA TN D-4777

EFFECT OF RESIDUAL STRESS ON FRACTURE STRENGTH OF AISI 301 STAINLESS-STEEL AND Ti-5Al-2.5Sn ELI TITANIUM CRACKED THIN-WALL CYLINDERS

By Frederick D. Calfo

Lewis Research Center
Cleveland, Ohio

NATIONAL AERONAUTICS AND SPACE ADMINISTRATION

For sale by the Clearinghouse for Federal Scientific and Technical Information
Springfield, Virginia 22151 – CFSTI price $3.00

ABSTRACT

Six-inch- (15.2-cm-) diameter cylinders containing through-cracks were fabricated from 0.020-inch- (0.051-cm-) thick Ti-5Al-2.5Sn ELI titanium and 0.022-inch- (0.056-cm-) thick AISI 301 stainless steel. Stress-relieved and non-stress-relieved cylinders were pressurized to burst at -423° and -320° F (20 and 77 K). The residual bending stresses in the titanium alloy were reduced from 65 000 to 6000 psi (45 000 to 4000 N/cm^2) by means of a stress-relieving heat treatment. The effect was an increase in fracture strength of about 10 000 to 15 000 psi (6900 to 10 400 N/cm^2). A reduction of residual stresses from 60 000 to 30 000 psi (42 000 to 21 000 N/cm^2) in the stainless-steel cylinders did not appreciably change their fracture strength.

EFFECT OF RESIDUAL STRESS ON FRACTURE STRENGTH OF AISI 301 STAINLESS-STEEL AND Ti-5Al-2.5Sn ELI TITANIUM CRACKED THIN-WALL CYLINDERS

by Frederick D. Calfo

Lewis Research Center

SUMMARY

Experimental data are presented to show the effect of residual stresses on the strength of 6-inch- (15.2-cm-) diameter cylindrical pressure vessels fabricated from flat sheet. Specimens were formed from nominally 0.022-inch- (0.056-cm-) thick AISI 301 stainless-steel 60 percent cold-reduced material and were tested at -423° F (20 K). Specimens were also formed from nominally 0.020-inch- (0.051-cm-) thick extra-low-interstitial (ELI) grade of the titanium alloy Ti-5Al-2.5Sn and were tested at -320° and -423° F (77 and 20 K). Specimens were either in a partially stress-relieved or non-stress-relieved condition and contained through-thickness fatigue cracks ranging from 0.15 to 1.5 inches (0.38 to 3.8 cm) in length.

The residual bending stresses introduced during the fabrication of the titanium alloy were reduced from 65 000 to 6000 psi (45 000 to 4000 N/cm^2) through heat treatment. The effect was an increase in the fracture strength of about 10 000 to 15 000 psi (6900 to 10 400 N/cm^2) independent of initial crack length. The combination of annealing and a reduction of residual stresses from 60 000 to 30 000 psi (42 000 to 21 000 N/cm^2) in the stainless-steel cylinders did not appreciably change their fracture strength.

INTRODUCTION

Pressure vessels are often fabricated by starting with flat sheet material and producing the required curvature in the sheet by one of a number of forming methods. Most of the methods result in the retention of residual stresses in the formed sheet. In some cases, the magnitude of the residual stresses can be an appreciable percentage of the yield or ultimate strength of the material. In the case of vessels containing flaws, the stress distribution in the vicinity of the flaw caused by pressure or external loading is

modified by the presence of residual stresses. Because the propagation of a flaw is dependent on the stress at the tip of the flaw, the strength of the vessel should be influenced by the residual stresses. It is important, therefore, to investigate the effect of residual stresses on the strength of vessels containing flaws and to determine associated material and temperature effects.

Pressure vessels with small radii of curvature have higher residual stresses than those with larger radii if they are made from flat sheet of the same thickness and are not subjected to an annealing or stress-relieving process. Thus, if material properties determined for scaled-down test tanks are to be applied to larger vessels, the effect of the residual stresses on the results should be determined. Also, the effect of stress-relief treatment on the failure pressures or stresses in tanks containing flaws is of interest.

Information is available concerning residual stresses and their effect on structures which have been formed by bending (refs. 1 to 3). However, very little information is available which accounts for the influence of residual stresses on the strength of vessels containing flaws.

A research program was therefore conducted at the Lewis Research Center to obtain some insight into the effect of residual stress on the fracture strength of vessels containing through-cracks. Scale model tanks were fabricated from flat sheet of two materials, AISI 301 stainless steel 60 percent cold-reduced and Ti-5Al-2.5Sn ELI titanium. These tanks, containing through-cracks of various lengths, were pressurized to the burst point. The 301 stainless-steel tanks were tested in the non-stress-relieved and 50 percent stress-relieved conditions. The Ti-5Al-2.5Sn ELI alloy tanks were tested in the non-stress-relieved condition. These results are compared with stress-relieved data obtained in a previous investigation using the same heat of material (ref. 4). In addition to the experimental work, an attempt was made to predict burst strength by using an analysis suggested by Robert B. Anderson (appendix). The analysis incorporates the effects of both residual stress and bulging in the vicinity of the flaw caused by internal pressure.

TEST SPECIMENS

AISI 301 Stainless-Steel Spiral-Welded Tanks

The pressure vessels which were fabricated from AISI 301 stainless-steel 60 percent cold-reduced material were formed by spiral wrapping nominally 0.022-inch- (0.056-cm-) thick sheet to form an 11° helix which was then butt-welded (see fig. 1). The cylinders were nominally 6 inches (15.2 cm) in diameter and 18 inches (45.7 cm) in length. The mill analysis of this material as furnished by the material supplier is given in table I. Specimens which were stress-relieved were heated for 8 hours at 750° F (673 K) and furnace cooled.

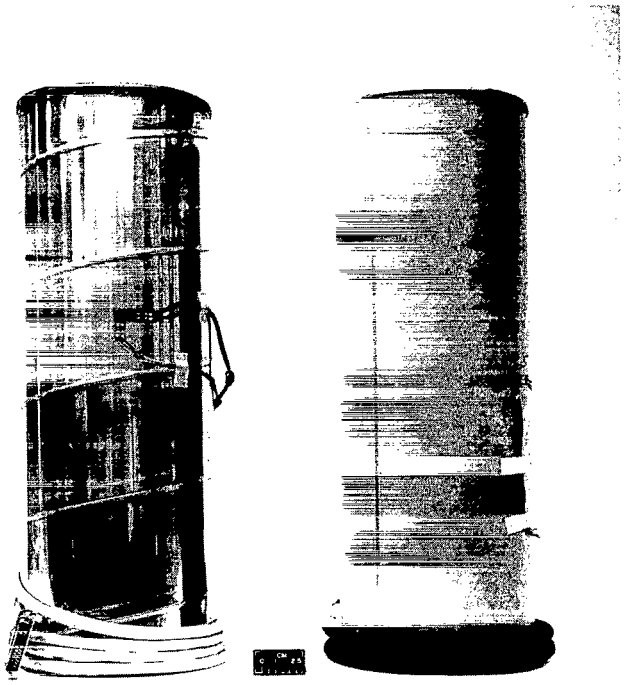

C-68-1141

Figure 1. - AISI 301 stainless-steel spiral-welded and titanium pressure vessels.

Ti-5Al-2.5Sn ELI Titanium Tanks

The Ti-5Al-2.5Sn ELI tanks were also 6 inches (15.2 cm) in diameter and 18 inches (45.7 cm) in length and were fabricated from nominally 0.020-inch- (0.051-cm-) thick sheet using a single longitudinal butt weld (fig. 1). The material was mill annealed at 1325^{o} F (991 K) for 4 hours and furnace cooled. The stress-relieved specimens were heated at 1100^{o} F (867 K) for 2 hours and furnace cooled. The chemical analysis of this alloy is also given in table I.

AISI 301 Stainless-Steel Uniaxial Specimens

The AISI stainless-steel 60 percent cold-reduced smooth and cracked tensile specimens shown in figure 2 were tested to determine the uniaxial tensile properties. Heat-treated and non-heat-treated specimens were tested at -423^{o} F (20 K). Non-heat-treated specimens were tested at -320^{o} and 70^{o} F (77 and 294 K). The test data were obtained from the same sheet stock as that used for the test cylinders. The direction of loading

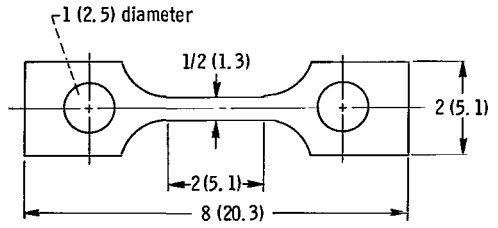

(a) Smooth specimen.

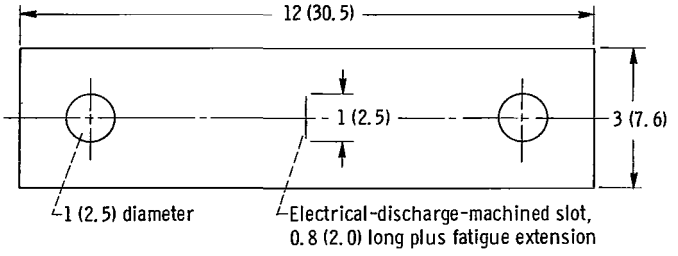

(b) Center-cracked specimen.

Figure 2. - Sheet specimens. (All dimensions in inches (cm).)

corresponded to an angle of 11° to the rolling direction of the sheet material. This direction corresponds to the hoop direction in the spiral-wound tanks. Each specimen contained a nominally 1-inch (2.5-cm) central crack. Slots were made by using the same machining method as that used for the tanks; this method is indicated in the section APPARATUS AND PROCEDURE. Cracks were made by low-stress-fatiguing the slot to the desired crack length. When testing to failure, an antibuckling fixture was applied to the surface of each cracked specimen to prevent buckling of the crack lips out of the plane of the sheet.

APPARATUS AND PROCEDURE

Residual Stress Measurement

The magnitudes of the residual stresses in the non-stress-relieved tanks and those remaining in the stress-relieved tanks had to be determined if they were to be considered analytically. Two measurement techniques were used to determine the magnitude of residual stress. The first method consisted of mounting foil strain gages on the outer surface of a hoop sample cut from the fabricated cylinder. By cutting the sample longitudinally it was possible to measure the relaxed strain, and thereby calculate the residual stresses which were relieved.

The second technique for determining residual stress involved measuring the change in curvature of the cylinder following the relaxation of residual stress in a tank sample and subsequent analytical determination of the stress. Hoop samples were again slit longitudinally and the new radius of curvature determined. The change in curvature is used in the following equation (ref. 2) to calculate the stress at the outer surface of the cylinder:

$$\sigma_r = \frac{Et}{2(1 - \mu^2)} \left(\frac{1}{r_o} - \frac{1}{r_f} \right) \tag{1}$$

where E is Young's modulus, t is the thickness, μ is Poisson's ratio for material, r_o is the radius of the hoop before slitting, and r_f is the radius of curvature after slitting. Equation (1) is based on a linear distribution of stress through the thickness of the material. Although this is an approximation, the values obtained for residual stresses are believed to be reasonably accurate. The values of E and μ used in the calculations are given in tables II and IV.

Fatigue Cracking

Machined slots. - To obtain experimental data relating flaw size to critical hoop stress, the tanks were provided with various-length through-slots, oriented longitudinally and, therefore, normal to the maximum principal stress. The slots were introduced by electrical discharge machining. The slots in the 301 stainless-steel specimens ranged in length from 0.60 to 1.30 inches (1.53 to 3.29 cm); those in the titanium tanks varied from 0.15 to 1.30 inches (0.38 to 3.29 cm).

Fatigue-cracking machine. - Following the machining of the through-slot, each cylinder was assembled in a fatigue-cracking machine. The rig, which is shown in figure 3, uses hydraulic pressure to low-stress cycle the cylinder until the slot is fatigue-cracked to the desired length. In order to pressurize the cylinder, the through-slot was sealed with a composite patch and end closures were fastened into position with an alloy having a melting point of about 300° F (422 K). A description of the patching and end closure procedure is given in the section Experimental Procedure.

Control of fatigue crack. - The crack length was controlled during low-stress cycling by using a single-element foil gage. The gage was mounted on the surface of the specimen near the slot tip and perpendicular to the expected direction of crack growth. As the fatigue crack propagates it eventually breaks the single element. When the element is broken, an open circuit occurs which causes the fatigue rig to shut down. By placing the gage at the appropriate position, the desired crack length was obtained. The stress

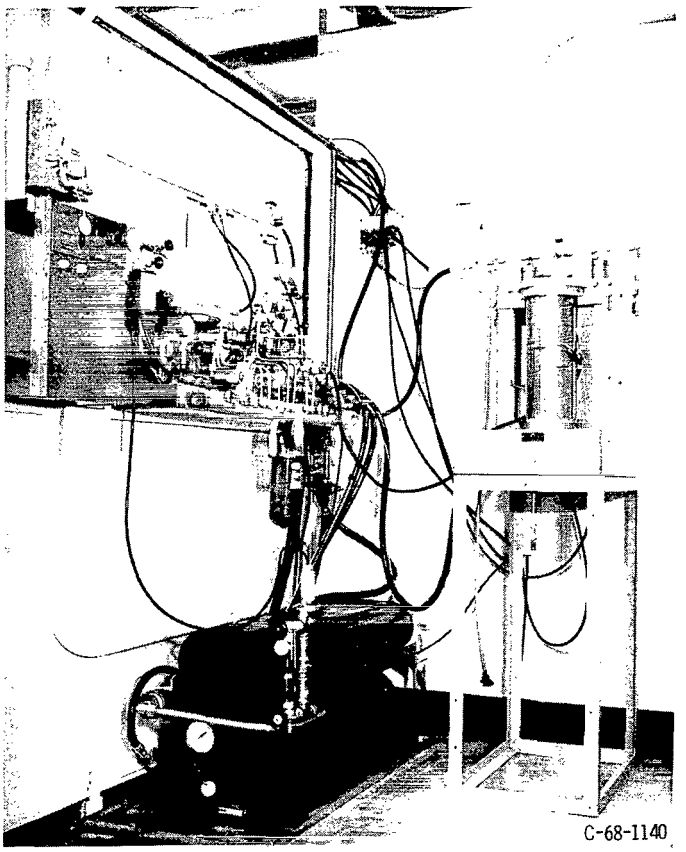

Figure 3. - Fatigue-crack-initiation rig.

level for cycling varied inversely with the desired crack length, as may be seen in tables V and VI for each specimen tested. The maximum cycle rate approached 1 cycle per second. Control of low-stress cycling was accomplished remotely; the cycle rate and upper and lower pressure levels were monitored by remote readout equipment.

Spiral-weld-heat-affected zone. - Cracks with lengths greater than 1 inch (2.54 cm) were located with their centers at the spiral weld in the 301 stainless-steel tanks. Thus, the possibility of the crack growth extending into the weld-heat-affected zone was avoided. Crack growth into the heat-affected zone would be expected to affect the failure strength of the tank. An investigation of the heat-affected zone not unexpectedly disclosed that a shrinkage stress existed in the region of the spiral weld and decreased rapidly on both sides of the weld. The zone extended approximately 0.125 inch (0.318 cm) on either side of the weld centerline.

Test Instrumentation

Following the low-stress cycling to fatigue-crack each tank, NASA electrical resistance continuity gages were mounted on the surface of each specimen to measure subcritical crack growth. These multiple-element foil gages were mounted at the tip of the crack, so that the parallel elements were perpendicular to the expected direction of crack growth. The gage elements were connected in parallel so that, as the crack grew through each element, finite resistance changes occurred. The resistance changes were monitored on read-out equipment and subsequently related to crack growth. A full description of the mounting methods and application of NASA continuity gages is presented in reference 5.

Experimental Procedure

To prevent contamination of, and possible explosive damage to, the cryogenic test facility, each cylinder was completely disassembled and thoroughly cleaned following the fatigue-cracking process.

Before testing the cylinders in liquid hydrogen or liquid nitrogen, it was again necessary to close the cylinder ends and seal the through-crack. The seal used was a composite patch designed to ensure proper sealing without reinforcing the area surrounding the crack. A layer of 0.002-inch (0.005-cm) Mylar pressure-sensitive tape was placed over the crack from inside the tank. A piece of 0.010-inch (0.025-cm) Mylar material was placed over the layer of tape. To prevent leaking during pressurization or local effects on the crack, the Mylar patch was made large enough to cover the original crack plus an additional amount to allow for stable crack growth. Three additional overlapping layers of Mylar tape completed the patch.

A cylindrical insert which reduced the volume of liquid hydrogen used in the test tank is described in reference 6. This insert minimized damage to the test specimen and test facility at failure. After assembly, the specimen was placed in a cryostat, submerged in and filled with the desired cryogen, and pressurized to burst. Gaseous helium was used as the pressurizing medium. A complete description of the test facility and the methods employed to decrease the hazards involved in a liquid-hydrogen test are presented in reference 7.

RESULTS AND DISCUSSIONS

Residual Stresses

The stress-relieving treatment used on the titanium alloy reduced residual stresses 90 percent or from approximately 65 000 to 6000 psi (45 000 to 4000 N/cm^2). The stress-relieving treatment used on the AISI 301 stainless-steel 60 percent cold-reduced material reduced residual stresses from approximately 60 000 to 30 000 psi (42 000 to 21 000 N/cm^2). These values were obtained by using the change in curvature technique and were within 10 percent of the values obtained by using the foil strain-gage method.

Results of Stainless-Steel Uniaxial Tests

The smooth and notched tensile properties of the AISI 301 stainless-steel material are listed in tables II and III. Tests were conducted at -423°, -320°, and 70° F (20, 77, and 294 K) for non-stress-relieved specimens. Stress-relieved specimens were tested at -423° F (20 K). In most cases three specimens were tested at each condition. The effect of stress-relieving was to decrease the yield and ultimate strength. The average yield strength value for the non-stress-relieved specimens was 265×10^3 psi (183×10^3 N/cm^2). Comparing this to an average value of 237×10^3 psi (163×10^3 N/cm^2) for the stress-relieved specimen results in a 10.6 percent variation. The average ultimate strength did not change significantly when the material was stress-relieved.

An examination of the notch test data listed in table III shows that the nominal fracture toughness decreased from an average value of 155×10^3 psi (170×10^3 N/cm^2) to 152×10^3 psi (167×10^3 N/cm^2) when stress-relieved, which is a 2 percent variation. Contrary to the nominal toughness, an increase in fracture toughness from 172×10^3 to 188×10^3 psi (189×10^3 to 206×10^3 N/cm^2) (a 9 percent change) occurred when specimens were stress-relieved. It is believed that in some cases the critical crack length may have been overestimated by the continuity gage due to a phenomenon called "catastrophic shear." This phenomenon is discussed by Wessel in reference 8. The effect of catastrophic shear on the accuracy of the continuity-gage-indicated crack length is discussed in reference 5.

Results of Burst Tests

The failure strength of a pressure vessel in the presence of a flaw is related to crack length and stress level through a material property called the critical stress in-

tensity factor, or fracture toughness. For through-cracks in thin infinite sheets, the plane stress fracture toughness is given by (ref. 9)

$$K_c = \sigma\sqrt{\pi a} \tag{2}$$

where σ is the gross stress normal to the plane of the crack and a is the critical half-crack length. Nominal fracture toughness based on initial half-crack length a_o is given by

$$K_{cn} = \sigma\sqrt{\pi a_o} \tag{3}$$

A dimensional analysis containing a dimensionless bulge coefficient C was derived in reference 4 to predict failure stresses in pressure vessels with through-cracks. The expression takes into account the increase in stress intensity due to bulging around the crack and plasticity at the crack tips. This concept has been extended in the appendix to include the effect of residual stress on fracture strength of cylindrical pressure vessels. The analysis thus estimates the decrease in strength of the pressurized cylinders by introducing a bulge coefficient C and a residual stress coefficient A to determine the hoop fracture strength.

In order to use the analysis, the critical hoop stress must first be determined from equation (A12) after the coefficients A and $\overline{C}$ have been empirically evaluated. Since the pressure vessels tested in this study contained two levels of residual stress for each material, a statistical method employing a regression analysis was developed in an attempt to find the bulge and residual stress coefficients.

Application of the statistical method to the existing data resulted in unrealistic values for both A and C. Since both coefficients are very sensitive to error, many more data points would probably have been necessary to obtain meaningful values.

Figures 4(a) and (b) (non-stress-relieved data listed in table V) present the fracture strength of Ti-5Al-2.5Sn ELI titanium alloy pressurized cylinders as a function of initial crack length. In figure 4(a), for the titanium alloy tested at -320° F (77 K) the effect of the stress-relieving treatment is an increase in the hoop fracture stress of 10 000 to 15 000 psi (6900 to 10 400 N/cm^2) independent of initial crack length. This increase in failure stress is only 20 to 30 percent of the bending stress which was relieved. This same phenomenon takes place at -423° F (20 K), as shown in figure 4(b).

The residual stresses which were relieved were due to bending; therefore, the maximum stress existed only at the outer surface and decreased rapidly through the thickness. At the outer surface the metal is subject to the least amount of constraint. It can yield more easily in that region than, for instance, at the middle surface. Consequently, it is reasonable that there is not a one-to-one correspondence between the

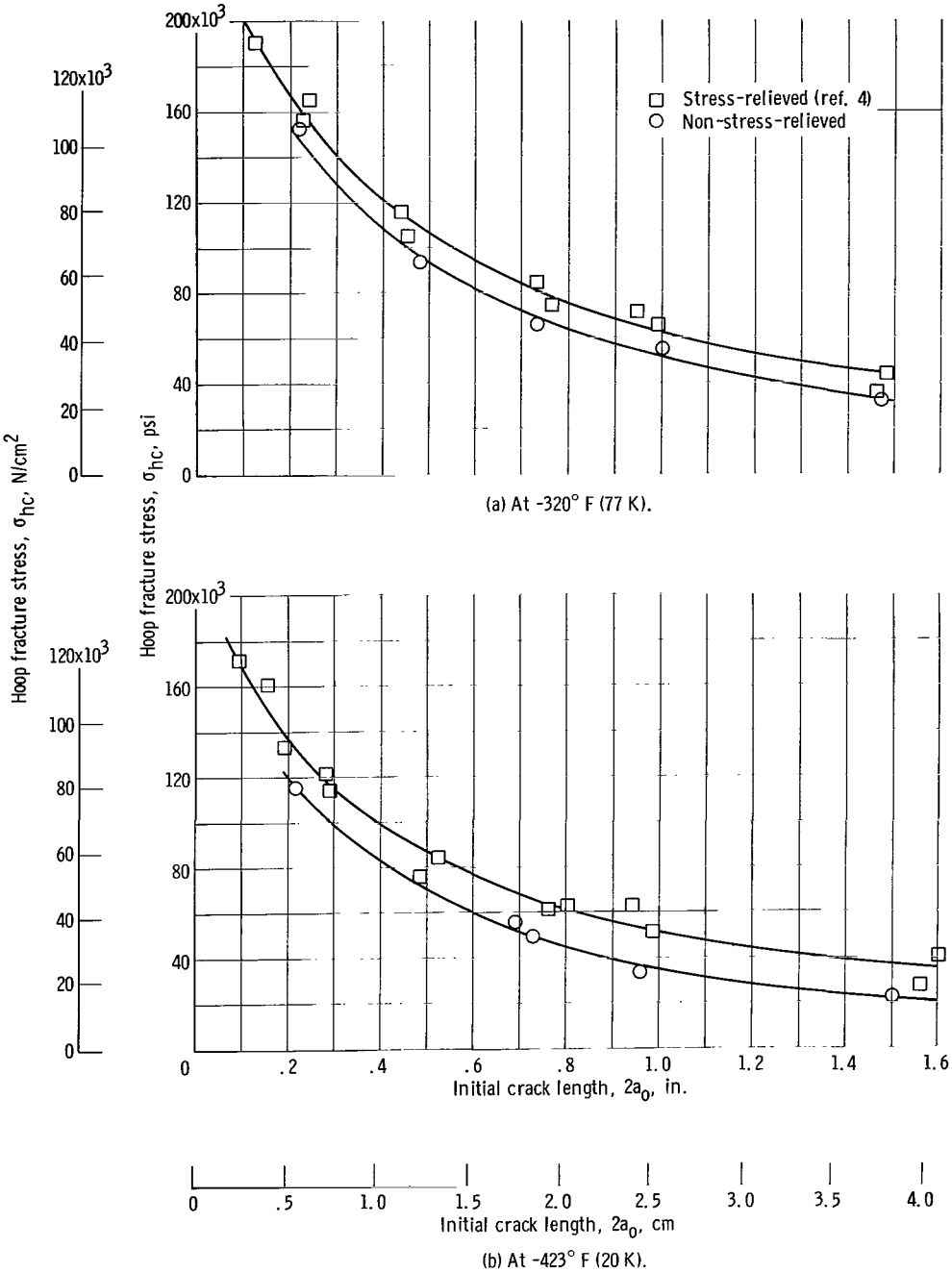

Figure 4. - Effect of initial crack length and stress relief on hoop fracture stress of Ti-5Al-2.5Sn ELI titanium pressure vessels. Diameter, 6.0 inches (15.2 cm); thickness, 0.020 inch (0.051 cm).

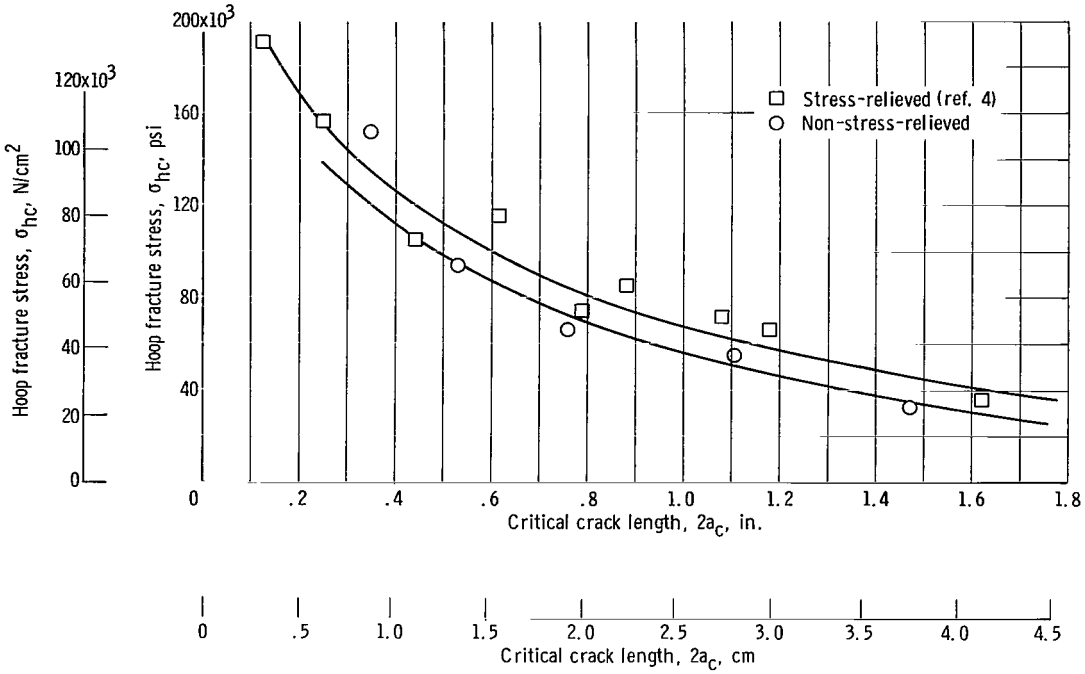

Figure 5. - Effect of critical crack length and stress relief on hoop fracture stress of Ti-5Al-2.5Sn ELI titanium pressure vessels at -320° F (77 K). Diameter, 6.0 inches (15.2 cm); thickness, 0.020 inch (0.051 cm).

residual stress present and the decrease in burst strength of the vessels. However, the 10 000- to 15 000-psi (6900- to 10 400-N/cm^2) decrease in burst strength due to residual stress is very significant even though it is only 20 to 30 percent of the residual stress.

Figure 5 (non-stress-relieved data listed in table V) is a plot of fracture stress against critical crack length (as opposed to initial crack length in fig. 4) for the titanium alloy tested at -320^o F (77 K). Thus, the crack growth which took place during pressurization of the cylinders and which was measured by continuity gages is accounted for in this plot.

Burst tests for the titanium alloy at -423^o F (20 K) showed no measurable subcritical crack growth; thus, the initial crack lengths presented in figure 4(b) are also the critical crack lengths.

Figures 6 and 7 (data listed in table VI) show fracture strength at -423^o F (20 K) of 301 stainless-steel 60 percent cold-reduced cylinders as a function of initial and critical crack length, respectively. Both figures show no variation in fracture strength between the non-stress-relieved and stress-relieved 301 stainless-steel tanks, even though the residual stresses in these cylinders were reduced about 50 percent, or from 60 000 to 30 000 psi (42 000 to 21 000 N/cm^2). The stress-relieving treatment also slightly annealed the material. Stress-relieving and annealing in combination probably compen-

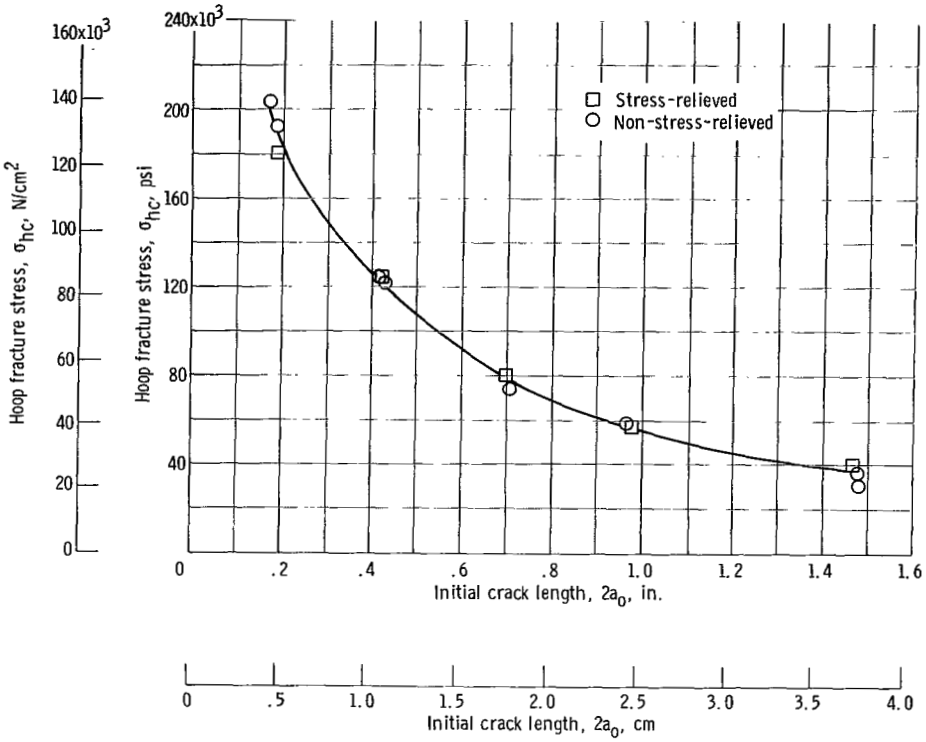

Figure 6. - Effect of initial crack length and stress relief on hoop fracture stress of AISI 301 stainless-steel 60 percent cold-reduced pressure vessels at -423° F (20 K). Diameter, 6.0 inches (15.2 cm); thickness, 0.022 inch (0.056 cm).

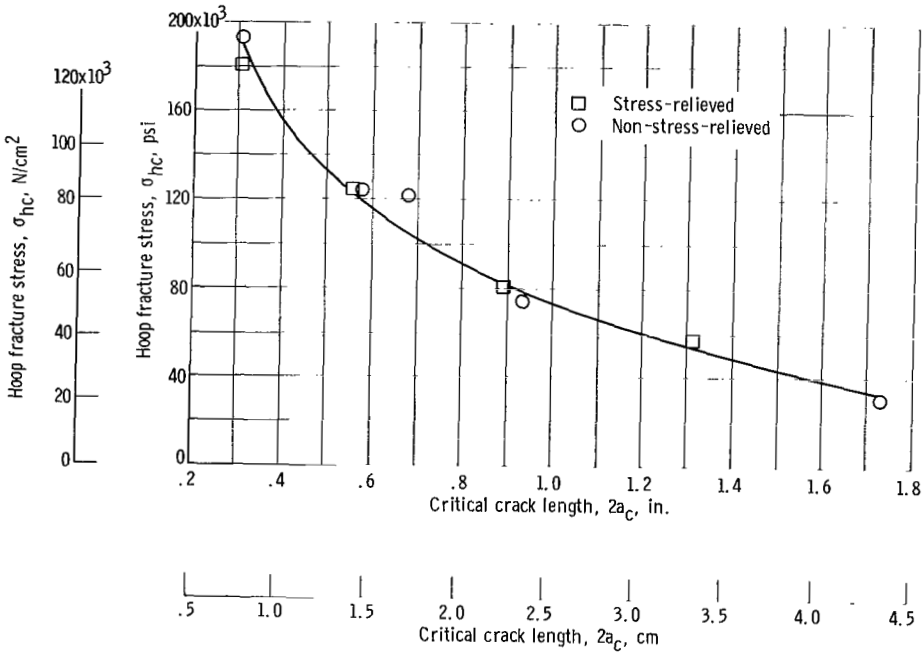

Figure 7. - Effect of critical crack length and stress relief on hoop fracture stress of AISI 301 stainless-steel 60 percent cold-reduced pressure vessels at -423° F (20 K). Diameter, 6.0 inches (15.2 cm); thickness, 0.022 inch (0.056 cm).

sated for each other and thus resulted in essentially no change in the fracture strength of the cylinders.

CONCLUDING REMARKS

Residual bending stresses due to roll-forming of 6-inch- (15.2-cm-) diameter cylinders were experimentally determined. In titanium alloy, Ti-5Al-2.5Sn ELI, cylinders fabricated from sheet (nominally 0.020 inch (0.051 cm) thick), the residual stress was approximately 65 000 psi (45 000 N/cm^2). In cylinders fabricated from AISI 301 stainless-steel, 60 percent cold-reduced sheet (nominally 0.022 inch (0.056 cm) thick), the residual stress was approximately 60 000 psi (42 000 N/cm^2).

Burst tests at -320° and -423° F (77 and 20 K) of titanium cylinders containing through-cracks ranging in length from $\frac{1}{4}$ to $1\frac{1}{2}$ inches (0.64 to 3.8 cm) showed that stress-relieving the cylinders increased the fracture strength about 10 000 to 15 000 psi (6900 to 10 400 N/cm^2) independent of the initial crack length. This increase in strength was about 20 to 30 percent of the bending stress relieved.

Burst tests at -423° F (20 K) of through-cracked stainless-steel cylinders in the non-stress-relieved and 50 percent stress-relieved conditions showed the stress-relief treatment had no effect on the fracture strength of the cylinders. It is believed that the reduction in residual stress and the annealing effect of the stress-relief treatment compensated for each other, and thereby eliminated the beneficial effect normally expected from stress relieving.

Lewis Research Center,
National Aeronautics and Space Administration,
Cleveland, Ohio, June 14, 1968,
124-08-08-19-22.

APPENDIX - FRACTURE ANALYSIS FOR CRACKED, ROLL-FORMED, PRESSURIZED CYLINDERS

by Robert B. Anderson*

The stress intensity near a through-crack in a roll-formed, pressurized cylinder is influenced by three major loading components: circumferential membrane stress, local bending caused by pressure-bulging around the crack, and residual bending stress due to roll-forming. The use of stress intensity factors associated with each of these loading conditions for relating the fracture strength of roll-formed, pressurized cylinders to vessel geometry, material properties, and residual stress is discussed herein.

The stress condition near a crack caused by circumferential tension in the cylinder wall is assumed to be the same as that near a crack in a tensioned flat sheet. For this reason the elastic stress intensity factor related to circumferential membrane stress is considered to be that of an infinitely large flat sheet stressed uniformly in tension. The circumferential stress intensity factor is given in reference 4, as derived from the flat-sheet stress intensity factor of reference 9, in terms of the circumferential membrane stress σ_h and the plastically corrected half-crack length $\bar{a}$ by

$$K_h = \sigma_h \sqrt{\pi \bar{a}} \tag{A1}$$

The bending stress intensity factor associated with pressure-bulging around the crack is derived through a semiempirical dimensional analysis in reference 4 as

$$K_b = \sigma_h \sqrt{\pi \bar{a}}\ \bar{C}\ \frac{a}{R} \tag{A2}$$

in which a is half the crack length, R is the radius of the cylinder, and $\bar{C}$ is an empirical coefficient.

The stress intensity factor related to residual bending stress in the roll-formed cylinder is approximated by that of an infinitely large sheet subjected to uniform bending. The stress intensity factor due to a remote bending moment is given in reference 10 as

$$K_m = \sigma_o \sqrt{\pi a} \tag{A3}$$

in which σ_o is the remote stress in the surface layer of the sheet. When referred to a roll-formed cylinder, the residual bending stress intensity factor is given as

*Carnegie Mellon University, Pittsburgh, Pa.

$$K_r = \sigma_r \sqrt{\pi \bar{a}} \tag{A4}$$

in which σ_r is the residual bending stress in the outer surface of the cylinder. The total stress intensity factor is

$$K_t = K_h + K_b + K_r \tag{A5}$$

At this point the Griffith-Irwin fracture condition could be used to relate the critical pressure or critical circumferential stress to the crack length and the vessel geometry. This condition specifies that fracture occurs when the stress intensity factor (in this case, the opening mode stress intensity factor) attains or exceeds a critical value; that is,

$$\frac{K}{K_c} \geq 1 \tag{A6}$$

or, if referred to the outer-surface stress intensity factor of a pressurized, roll-formed cylinder,

$$\frac{K_h + K_b + K_r}{K_{tc}} \geq 1 \tag{A7}$$

In the absence of pressure-bulging and residual bending, the critical total stress intensity factor should be that of a flat sheet of equal thickness, namely, the fracture toughness K_c. Accordingly, K_{tc} must equal or exceed K_c so that the fracture condition of inequality (A7) becomes

$$\frac{K_h + K_b + K_r}{K_c} \geq 1 \tag{A8}$$

Then, from equations (1) to (3) and inequality (A8), the critical circumferential stress is

$$\sigma_{hc} = \frac{\dfrac{K_c}{\sqrt{\pi \bar{a}_c}} - \sigma_r}{1 + \bar{C} \dfrac{a}{R}} \tag{A9}$$

According to the condition specified by inequality (A8), for the special case of $K_h = 0$ the total bending stress intensity factor $K_b + K_r$ at fracture must equal the tensile fracture toughness K_c. However, experimental evidence is given in reference 11 that indicates, for pure bending of plexiglas sheet, the critical bending stress intensity factor K_{mc} is 2 to $2\frac{1}{2}$ times the tensile fracture toughness K_c. Although these relative toughness values are reported for only one material, the observation suggests that fracture under bending is not determined exclusively by the tensile stress intensity on the outer surface.

An interaction criterion relating critical bending and critical extensional stress intensity factors must be used to account for the observations of reference 11. The simplest interaction condition for fracture is the linear inequality

$$\frac{K_b + K_r}{K_{mc}} + \frac{K_h}{K_c} \geq 1 \tag{A10}$$

which reduces to inequality (A7) for $K_{mc} = K_c$. If the ratio K_c/K_{mc} is designated by A, the linear interaction fracture condition becomes

$$\frac{K_h + A(K_b + K_r)}{K_c} \geq 1 \tag{A11}$$

Accordingly, the critical circumferential stress is derived from equations (1) to (3) and inequality (A11) as

$$\sigma_{hc} = \frac{\dfrac{K_c}{\sqrt{\pi \bar{a}_c}} - A\sigma_r}{1 + A\bar{C}\,\dfrac{a}{R}} \tag{A12}$$

It is likely that the ratio A varies with material properties, sheet thickness, and environmental conditions. Hence, both A and $\bar{C}$ must be evaluated experimentally for specific materials in specific environments.

REFERENCES

1. Baldwin, W. M., Jr.: Residual Stresses in Metals. ASTM Proc., vol. 49, 1949, pp. 539-583.

2. Conway, H. D.; and Nickola, W. E.: Anticlastic Action of Flat Sheets in Bending. Paper No. 895, Soc. Exper. Stress Anal., 1964.

3. Osgood, William R., ed.: Residual Stresses in Metals and Metal Construction. Reinhold Publ. Corp., 1954.

4. Anderson, Robert B.; and Sullivan, Timothy L.: Fracture Mechanics of Through-Cracked Cylindrical Pressure Vessels. NASA TN D-3252, 1966.

5. Sullivan, Timothy L.; and Orange, Thomas W.: Continuity Gage Measurement of Crack Growth on Flat and Curved Surfaces at Cryogenic Temperatures. NASA TN D-3747, 1966.

6. Calvert, Howard F.; and Kemp, Richard H.: Determination of Pressure Vessel Strengths at -423^{o} F as Influenced by Notches of Various Radii. Paper No. 520 B, SAE, Apr. 1962.

7. Getz, David L.; Pierce, William S.; and Calvert, H. F.: Correlation of Uniaxial Notch Tensile Data with Pressure Vessel Fracture Characteristics. Paper No. 63-WA-187, ASME, 1963.

8. Wessel, E. T.: Some Exploratory Observations of the Tensile Properties of Metals at Very Low Temperatures. ASM Trans., vol. 49, 1957, pp. 149-172.

9. ASTM Special Committee on Fracture Toughness Testing of High-Strength Metallic Materials: Fracture Testing of High-Strength Sheet Materials. Part I. Bull. No. 243, ASTM, 1960, pp. 29-40.

10. Paris, Paul C.; and Sih, George C.: Stress Analysis of Cracks. Fracture Toughness Testing and Its Applications. Spec. Tech. Publ. No. 381, ASTM, 1965, pp. 30-83.

11. Erdogan, Fazil; Tuncel, Ozcan; and Paris, Paul C.: An Experimental Investigation of the Crack Tip Stress Intensity Factor in Plates Under Cylindrical Bending. J. Basic Eng., vol. 84, no. 4, Dec. 1962, pp. 542-546.

12. Sullivan, Timothy L.: Uniaxial and Biaxial Fracture Toughness of Extra-Low-Interstitial 5Al-2.5Sn Titanium Alloy Sheet at 20^{o} K. NASA TN D-4016, 1967.

13. Sullivan, Timothy L.: Texture Strengthening and Fracture Toughness of Titanium Alloy Sheet at Room and Cryogenic Temperatures, NASA TN D-4444, 1968.

TABLE I. - MATERIAL COMPOSITION

Material	Heat	Composition, wt. %						
AISI 301 stainless steel, 60 percent cold-reduced[a]	348 524	C	P	S	Si	Cr	Ni	Mn
		0.11	0.23	0.009	0.60	17.26	7.10	1.44
Ti-5Al-2.5Sn ELI[b]	D-3272	C	Fe	N	Al	H	O	Sn	Mn
		0.022	0.08	0.014	5.1	0.006 to 0.009	0.08	2.5	0.006

[a]Those specimens which were stress-relieved were heated at 750° F (672 K) for 8 hr and furnace cooled.

[b]Sheet was annealed at 1325° F (991 K) for 4 hr and furnace cooled. After fabrication, specimens which were stress-relieved were heated at 1100° F (867 K) for 2 hr and furnace cooled.

TABLE II. - SMOOTH PROPERTIES OF AISI 301 STAINLESS STEEL, 60 PERCENT COLD-REDUCED, STRESS-RELIEVED AND NON-STRESS-RELIEVED

[Angle to rolling direction, 11°.]

(a) U. S. Customary Units

Temperature, °F	Stress relieved[a]	0.2 percent yield strength, psi	Ultimate strength, psi	Modulus of elasticity, E, psi
70	No	217×10^3	239×10^3	24.3×10^6
		212	231	24.6
		216	238	24.3
Average		215×10^3	236×10^3	24.4×10^6
-320	No	234×10^3	331×10^3	28.8×10^6
		242	329	26.3
		243	328	27.4
Average		239×10^3	329×10^3	27.5×10^6
-423	No	257×10^3	324×10^3	28.8×10^6
		275	321	25.7
		263	324	26.9
		267	320	26.3
Average		265×10^3	322×10^3	26.9
-423	Yes	241×10^3	329×10^3	28.3×10^6
		232	327	28.5
		237	324	29.6
Average		237×10^3	327×10^3	28.8×10^6

(b) SI Units

Temperature, K	Stress relieved[a]	0.2 percent yield strength, N/cm^2	Ultimate strength, N/cm^2	Modulus of elasticity, E, N/cm^2
294	No	149×10^3	165×10^3	16.7×10^6
		146	159	16.9
		149	164	16.7
Average		148×10^3	163×10^3	16.8×10^6
77	No	161×10^3	228×10^3	19.8×10^6
		167	227	18.1
		167	226	18.9
Average		165×10^3	227×10^3	18.9×10^6
20	No	177×10^3	223×10^3	19.8×10^6
		189	221	17.7
		181	223	18.5
		184	220	18.1
Average		183×10^3	222×10^3	18.5×10^6
20	Yes	166×10^3	227×10^3	19.5×10^6
		160	225	19.6
		163	223	20.4
Average		163×10^3	225×10^3	19.8×10^6

[a]Heat treated at 750° F (672 K) for 8 hr.

TABLE III. - NOTCH PROPERTIES OF AISI 301 STAINLESS STEEL, 60 PERCENT COLD-REDUCED, STRESS-RELIEVED AND NON-STRESS-RELIEVED

[Angle to rolling direction, 11°.]

(a) U. S. Customary Units

Temperature, °F	Stress relieved[a]	Thickness, in.	Initial crack length, in.	Critical crack length, in.	Gross fracture stress, psi	Net fracture stress, psi	Nominal fracture toughness, psi $\sqrt{in.}$	Fracture toughness, psi $\sqrt{in.}$
-320	No	0.0228	1.024	1.30	110×10^3	168×10^3	160×10^3	192×10^3
		.0228	1.039	1.33	111	170	162	196
		.0229	1.027	1.32	110	168	160	195
		Average			110×10^3	169×10^3	161×10^3	194×10^3
-423	No	0.0227	1.024	1.13	106×10^3	162×10^3	150×10^3	161×10^3
		.0228	1.024	1.26	110	169	157	183
		0229	1.028	1.16	110	169	158	172
		Average			109×10^3	167×10^3	155×10^3	172×10^3
-423	Yes	0.0226	1.024	1.25	107×10^3	163×10^3	154×10^3	178×10^3
		.0225	1.011	1.36	105	159	149	188
		.0226	1.012	1.39	107	162	153	196
		Average			106×10^3	162×10^3	152×10^3	188×10^3

(b) SI Units

Temperature, K	Stress relieved[a]	Thickness, cm	Initial crack length, cm	Critical crack length, cm	Gross fracture stress, N/cm^2	Net fracture stress, N/cm^2	Nominal fracture toughness, $(N/cm^2)\sqrt{cm}$	Fracture toughness, $(N/cm^2)\sqrt{cm}$
77	No	0.0579	2.601	3.30	76.0×10^3	116×10^3	176×10^3	211×10^3
		.0579	2.639	3.38	76.1	117	178	215
		.0582	2.609	3.36	76.0	116	176	214
		Average			76.1×10^3	116×10^3	177×10^3	213×10^3
20	No	0.0577	2.601	2.87	72.9×10^3	112×10^3	165×10^3	177×10^3
		.0579	2.601	3.20	75.9	117	173	201
		.0582	2.611	2.95	75.9	117	173	189
		Average			74.9×10^3	115×10^3	170×10^3	189×10^3
20	Yes	0.0574	2.601	3.16	73.4×10^3	112×10^3	169×10^3	196×10^3
		.0572	2.568	3.45	72.0	110	164	206
		.0574	2.570	3.52	73.4	112	168	216
		Average			72.9×10^3	111×10^3	167×10^3	206×10^3

[a]Heat treated at 750° F (672 K) for 8 hr.

TABLE IV. - SUMMARY OF AVERAGE TEST DATA AND MATERIAL COEFFICIENTS

(a) U. S. Customary Units

Material	Temperature, °F	0.2 percent yield strength, psi	Ultimate strength, psi	2 to 1 biaxial yield strength, psi	Fracture toughness, K_c, psi$\sqrt{\text{in.}}$	Nominal fracture toughness, K_{cn}, psi$\sqrt{\text{in.}}$	Elastic Poisson's ratio, μ	Modulus of elasticity, E, psi
Ti-5Al-2.5Sn ELI titanium, stress-relieved and non-stress-relieved	-423	[a] 204×10^3	[a] 226×10^3	[b] 252×10^3	[a] 103×10^3	[b] 87.5×10^3	[c] 0.380	[a] 17.7×10^6
	-320	[a] 173×10^3	[a] 180×10^3	[b] 222×10^3	[b] 160×10^3	[b] 139×10^3	[c] .390	[a] 18.1×10^6
AISI 301 stainless steel, 60 percent cold-reduced	Stress-relieved							
	-423	237×10^3	327×10^3	272×10^3 (assumed)	188×10^3	152×10^3	0.30 (assumed)	28.8×10^6
	Non-stress-relieved							
	-423	265×10^3	322×10^3	305×10^3	172×10^3	155×10^3	0.30 (assumed)	26.9×10^6

(b) SI Units

Material	Temperature, K	0.2 percent yield strength, psi N/cm^2	Ultimate strength, psi N/cm^2	2 to 1 biaxial yield strength, N/cm^2	Fracture toughness, K_c, $(N/cm^2)\sqrt{cm}$	Nominal fracture toughness, K_{cn}, $(N/cm^2)\sqrt{cm}$	Elastic Poisson's ratio, μ	Modulus of elasticity, E, N/cm^2
Ti-5Al-2.5Sn ELI titanium, stress-relieved and non-stress-relieved	20	[a] 140×10^3	[a] 156×10^3	[b] 174×10^3	[a] 113×10^3	[b] 96.2×10^3	[c] 0.380	[a] 12.2×10^6
	77	[a] 119×10^3	[a] 124×10^3	[b] 153×10^3	[b] 176×10^3	[b] 153×10^3	[c] .390	[a] 12.5×10^6
AISI 301 stainless steel, 60 percent cold-reduced	Stress-relieved							
	20	163×10^3	225×10^3	188×10^3 (assumed)	206×10^3	167×10^3	0.30 (assumed)	19.8×10^6
	Non-stress-relieved							
	20	183×10^3	222×10^3	210×10^3	189×10^3	170×10^3	0.30 (assumed)	18.5×10^6

[a] Ref. 12.
[b] Ref. 4.
[c] Ref. 13.

TABLE V. - GEOMETRY AND TEST DATA FOR Ti-5Al-2.5Sn ELI TITANIUM ALLOY,

6-INCH- (15.2-CM-) DIAMETER NON-STRESS-RELIEVED SPECIMENS

[Minimum stress for cyclic loading to fatigue crack, 1.4×10^3 psi (0.97×10^3 N/cm^2).]

(a) U.S. Customary Units

Temperature, °F	Radius, in.	Thickness, in.	Slot length, in.	Initial crack length, in.	Critical crack length, in.	Cycles to fatigue crack	Cyclic loading to fatigue crack, maximum stress, psi	Hoop stress at failure due to internal pressure, psi
-423	3.00	0.0198	0.15	0.215	----	6130	36.4×10^3	115×10^3
	3.01	.0194	.30	.690	----	6900	27.2	55.8
	3.00	.0190	.60	.728	----	[a]500 and 1600	[a]31.6×10^3 and 23.7×10^3	49.4
	3.02	.0176	.80	.957	----	2500	15.4×10^3	33.4
	3.00	.0198	1.30	1.501	----	5640	6.8	22.4
-320	3.00	0.0190	0.15	0.218	0.35	5300	33.2×10^3	152×10^3
	3.01	.0198	.30	.477	.53	7000	27.4	93.9
	3.00	.0191	.60	.732	.76	1700	23.6	66.0
	3.00	.0192	.80	1.001	1.11	5000	13.3	54.7
	3.01	.0203	1.30	1.471	1.48	6000	6.7	32.5

(b) SI Units

Temperature, K	Radius, cm	Thickness, cm	Slot length, cm	Initial crack length, cm	Critical crack length, cm	Cycles to fatigue crack	Cyclic loading to fatigue crack, maximum stress, N/cm^2	Hoop stress at failure due to internal pressure, N/cm^2
20	7.62	0.0503	0.38	0.546	----	6130	25.1×10^3	79.5×10^3
	7.65	.0493	.76	1.753	----	6900	18.7	38.5
	7.62	.0483	1.52	1.849	----	[a]500 and 1600	[a]21.8×10^3 and 16.3×10^3	34.0
	7.67	.0447	2.03	2.431	----	2500	10.6×10^3	23.0
	7.62	.0503	3.30	3.813	----	5640	4.7	15.4
77	7.62	0.0483	0.38	0.554	0.89	5300	22.9×10^3	105.0×10^3
	7.65	.0503	.76	1.212	1.35	7000	18.9	64.7
	7.62	.0485	1.52	1.859	1.93	1700	16.3	45.5
	7.62	.0488	2.03	2.537	2.82	5000	9.2	37.7
	7.65	.0516	3.30	3.736	3.76	6000	4.6	22.4

[a]Specimen cycled at two maximum stress levels.

TABLE VI. - GEOMETRY AND TEST DATA FOR AISI 301 STAINLESS-STEEL, 60 PERCENT COLD-REDUCED, 6-INCH- (15.2-CM-) DIAMETER TANKS

[Minimum stress for cyclic loading to fatigue crack, 1.4×10^3 psi.]

(a) U.S. Customary Units

Temperature, °F	Radius, in.	Thickness, in.	Slot length, in.	Initial crack length, in.	Critical crack length, in.	Cycles to fatigue crack	Cycling loading to fatigue crack, maximum stress, psi	Hoop stress at failure due to internal pressure, psi	Stress relieved
-423	3.01	0.0222	0.060	0.171	(a)	15 700	56.0×10^3	203×10^3	No
	3.00	.0221	.125	.188	0.30	[b]90 000 and 50 000	[b]13.6×10^3 and 20.5×10^3	193	
	3.01	.0223	.250	.416	.58	130 000	20.5×10^3	124	
	3.01	.0235	.350	.429	.68	1 400	45.7	121	
	3.01	.0230	.500	.706	.94	12 500	19.6	74.1	
	3.00	.0227	.800	.962	(c)	4 800	20.5	58.1	
	2.99	.0230	1.300	1.477	(c)	26 700	8.2	37.1	
	3.00	.0231	1.300	1.482	1.73	8 000	7.2	31.0	
	3.00	.0231	.125	.190	.30	53 000	20.9	181	Yes
	3.02	.0231	.350	.422	.55	2 400	39.1	125	
	3.01	.0210	.500	.696	.89	26 900	17.9	81.0	
	3.00	.0223	.800	.977	1.31	27 000	10.9	57.3	
	3.02	.0208	1.300	1.463	(c)	7 300	10.5	40.4	
-320	3.00	0.0225	0.060	0.161	0.25	11 000	61.4×10^3	202×10^3	No
	3.02	.0231	.125	.170	.28	10 900	45.7	196	
	3.02	.0220	.250	.390	(c)	39 000	23.9	133	
	3.01	.0233	.350	.472	(c)	1 900	52.2	126	
	3.01	.0234	.500	.720	.94	18 400	17.6	79.4	
	3.02	.0232	.800	.881	1.13	8 000	13.0	59.5	
	3.02	.0231	1.300	1.452	(a)	8 700	13.0	35.3	

[a]No crack growth indicated.

[b]Specimen cycled at two maximum stress levels.

[c]Insufficient continuity-gage data.

TABLE VI. - Concluded. GEOMETRY AND TEST DATA FOR AISI 301 STAINLESS-STEEL, 60 PERCENT COLD-REDUCED, 6-INCH- (15.2-CM-) DIAMETER TANKS

[Minimum stress for cyclic loading to fatigue crack, 0.97×10^3 N/cm^2.]

(b) SI Units

Temperature, K	Radius, cm	Thickness, cm	Slot length, cm	Initial crack length, cm	Critical crack length, cm	Cycles to fatigue crack	Cycling loading to fatigue crack, maximum stress, N/cm^2	Hoop stress at failure due to internal pressure, N/cm^2	Stress relieved
20	7.65	0.0564	0.152	0.434	(a)	15 700	38.6×10^3	140×10^3	No
	7.62	.0561	.318	.478	0.77	[b]90 000 and 50 000	[b]9.4×10^3 and 14.1×10^3	133	
	7.65	.0566	.635	1.057	1.46	130 000	14.1×10^3	85.6	
	7.65	.0597	.889	1.080	1.72	1 400	31.5	83.6	
	7.65	.0584	1.270	1.793	2.38	12 500	13.5	51.1	
	7.62	.0577	2.032	2.443	(c)	4 800	14.1	40.0	
	7.59	.0584	3.302	3.752	(c)	26 700	5.7	25.6	
	7.62	.0587	3.302	3.764	4.40	8 000	5.0	21.4	
	7.62	.0587	.318	.483	.77	53 000	14.4	124	Yes
	7.67	.0587	.889	1.077	1.41	2 400	26.9	86.1	
	7.65	.0533	1.270	1.768	2.27	26 900	12.3	55.8	
	7.62	.0566	2.032	2.482	3.33	27 000	7.5	39.5	
	7.67	.0528	3.302	3.726	(c)	7 300	7.2	27.8	
77	7.62	0.0572	0.152	0.409	0.63	11 000	42.3×10^3	139×10^3	No
	7.67	.0587	.318	.430	.71	10 900	31.5	135	
	7.67	.0559	.635	.991	(c)	39 000	16.5	91.3	
	7.65	.0592	.889	1.199	(c)	1 900	36.0	86.7	
	7.65	.0594	1.270	1.829	2.38	18 400	12.1	54.7	
	7.67	.0589	2.032	2.238	2.87	8 000	9.0	41.0	
	7.67	.0587	3.302	3.688	(c)	8 700	9.0	24.3	

[a]No crack growth indicated.

[b]Specimen cycled at two maximum stress levels.

[c]Insufficient continuity-gage data.

"The aeronautical and space activities of the United States shall be conducted so as to contribute . . . to the expansion of human knowledge of phenomena in the atmosphere and space. The Administration shall provide for the widest practicable and appropriate dissemination of information concerning its activities and the results thereof."

—NATIONAL AERONAUTICS AND SPACE ACT OF 1958

NASA SCIENTIFIC AND TECHNICAL PUBLICATIONS

TECHNICAL REPORTS: Scientific and technical information considered important, complete, and a lasting contribution to existing knowledge.

TECHNICAL NOTES: Information less broad in scope but nevertheless of importance as a contribution to existing knowledge.

TECHNICAL MEMORANDUMS: Information receiving limited distribution because of preliminary data, security classification, or other reasons.

CONTRACTOR REPORTS: Scientific and technical information generated under a NASA contract or grant and considered an important contribution to existing knowledge.

TECHNICAL TRANSLATIONS: Information published in a foreign language considered to merit NASA distribution in English.

SPECIAL PUBLICATIONS: Information derived from or of value to NASA activities. Publications include conference proceedings, monographs, data compilations, handbooks, sourcebooks, and special bibliographies.

TECHNOLOGY UTILIZATION PUBLICATIONS: Information on technology used by NASA that may be of particular interest in commercial and other non-aerospace applications. Publications include Tech Briefs, Technology Utilization Reports and Notes, and Technology Surveys.

Details on the availability of these publications may be obtained from:

SCIENTIFIC AND TECHNICAL INFORMATION DIVISION

NATIONAL AERONAUTICS AND SPACE ADMINISTRATION

Washington, D.C. 20546